



Antihypertensive Effect of a Novel Angiotensin II Receptor Blocker Fluorophenyl Benzimidazole: Contribution of cGMP, Voltage-dependent Calcium Channels, and BK_{Ca} Channels to Vasorelaxant Mechanisms

OPEN ACCESS

Edited by:

Bimal Malhotra,

Pfizer (United States), United States

Reviewed by:

Isac Medeiros,

Federal University of Paraíba, Brazil

Andrew P. Braun,

University of Calgary, Canada

*Correspondence:

Debabrata Chanda
chandapt@gmail.com

†These authors have contributed equally to this work.

Specialty section:

This article was submitted to Cardiovascular and Smooth Muscle Pharmacology, a section of the journal *Frontiers in Pharmacology*

Received: 28 September 2020

Accepted: 09 February 2021

Published: 30 March 2021

Citation:

Iqbal H, Verma AK, Yadav P, Alam S, Shafiq M, Mishra D, Khan F, Hanif K, Negi AS and Chanda D (2021) Antihypertensive Effect of a Novel Angiotensin II Receptor Blocker Fluorophenyl Benzimidazole: Contribution of cGMP, Voltage-dependent Calcium Channels, and BK_{Ca} Channels to Vasorelaxant Mechanisms. *Front. Pharmacol.* 12:611109. doi: 10.3389/fphar.2021.611109

Hina Iqbal^{1†}, Amit Kumar Verma^{2†}, Pankaj Yadav¹, Sarfaraz Alam³, Mohammad Shafiq⁴, Divya Mishra¹, Feroz Khan³, Kashif Hanif⁴, Arvind Singh Negi² and Debabrata Chanda^{1*}

¹Bioprospection and Product Development Division, CSIR-Central Institute of Medicinal and Aromatic Plants, Lucknow, India, ²Phytochemistry Division, CSIR-Central Institute of Medicinal and Aromatic Plants, Lucknow, India, ³Computational Biology Lab, CSIR-Central Institute of Medicinal and Aromatic Plants, Lucknow, India, ⁴Division of Pharmacology, CSIR-Central Drug Research Institute, Lucknow, India

Background: The current study presents the novel angiotensin II receptor blocker fluorophenyl benzimidazole (FPD) as an antihypertensive agent in the SHR model of hypertension. We investigated the role of cGMP, voltage-dependent L-type calcium channels, and BK_{Ca} channels in the vasorelaxant mechanisms of FPD in the rat superior mesenteric artery.

Methods: The antihypertensive effect of FPD was examined using an invasive technique measuring blood pressure in SHR animals. Using a myograph, tension measurement was completed in the superior mesenteric artery to elucidate the mechanisms of vasorelaxation involving AT1 receptors, the NO/cGMP pathway, L-type calcium channels, and BK_{Ca} channels. Ion flux (Ca²⁺, K⁺) studies were conducted in aortic smooth muscle cells. Putative targets proteins were determined by *in silico* docking studies. A safety evaluation of FPD was carried out using Swiss albino mice.

Results: FPD significantly decreased blood pressure in SHR. It relaxed superior mesenteric arteries in a concentration-dependent manner and significantly inhibited angiotensin II-induced contraction. The relaxation response was also mediated by an increase in tissue cGMP levels, inhibition of L-type calcium channels, and the opening of BK_{Ca} channels. FPD further enhanced efflux of K⁺ and inhibited Bay K8644-stimulated

Abbreviations: 4-AP, 4-aminopyridine; DAPI, 4',6'-diamidino-2-phenylindole; DMSO, dimethylsulfoxide; FPD, fluorophenyl benzimidazole; High K⁺ MKHS, high potassium depolarizing solution; L-NAME, N^ω-nitro-L-arginine methyl ester hydrochloride; MKHS, modified Krebs-Henseleit solution; ODQ, 1H-[1,2,4]oxadiazolo [4,3-a]quinoxalin-1-one; TCA, trichloroacetic acid; TEA, tetraethyl ammonium; U46619, thromboxane analogue.

Ca²⁺ influx in aortic smooth muscle cells and docked well in an *in silico* study with the targets. It was well tolerated in the toxicity study.

Conclusion: The present study reports the antihypertensive activity of novel AT-1 receptor blocker FPD at 50 and 100 mg kg⁻¹ with cGMP, L-type calcium channels, and BK_{Ca} channels as putative targets of vasorelaxation, and was found safe in oral toxicity.

Keywords: hypertension, benzimidazole, BK_{Ca} channel, L-type VDCC, SHRs, cGMP

INTRODUCTION

Non-communicable diseases are the leading cause of death in the developed and developing world. They are responsible for approximately 68% of all global deaths, out of which approximately 46.2% of deaths occur due to cardiovascular diseases worldwide (WHO, 2017). Benzimidazoles and substituted benzimidazoles have been used for various biological activities including hypertension since 1944 (Woolley, 1944). Over time and through active research interest, benzimidazoles have emerged as an important heterocyclic class of molecules due to their clinical use as drugs like omeprazole as an antiulcer treatment, albendazole as an antiparasitic, benoxaprofen as an anti-inflammatory, bendamutine as an antineoplastic treatment, astemizole as an antihistamine, and pimobendane as a calcium sensitizer, etc. (Supplementary Figure S1A) (Bansal and Silakari, 2012). Further, benzimidazole has often been used as an important basic core, especially for the development of antihypertensive agents. Telmisartan, candesartan, and azilsartan have emerged from this class of compounds as clinical drugs acting through the angiotensin receptor blockade (AT1). In spite of the vast number of studies on benzimidazoles and angiotensin receptor blockers (ARBs), literature on the role of these classes of compounds on VDCC and potassium channel functioning pertaining to vasorelaxation in conduit and resistance arteries and antihypertensive activity has been very limited. In the present study, we planned to create a phenyl ring at the C2 position of a benzimidazole core, instead of N-benzylbiphenyl as in candesartan and telmisartan, to obtain a small molecular weight pharmacophore. A fluorine group was also kept to create a high electron density for better interaction, similar to a H-bond acceptor, with the receptor protein. All the 2-arylbenzimidazole derivatives were evaluated for vasorelaxation and the most potent molecule, fluorophenyl benzimidazole was studied for antihypertensive activity and elucidation of its mechanism of action through blocking the AT1 receptor, cGMP buildup, and modulation of the BK_{Ca} channel and VDCC function.

MATERIALS AND METHODS

Chemical Synthesis

Synthesis of 2-(4'-Fluorophenyl)-1H-benzimidazole (34/FPD): o-Phenylenediamine (128 mg, 1.2 mmol) and 4-fluorobenzaldehyde (124 mg, 1.0 mmol) were taken in dry methanol (10 ml). To this reaction mixture, 1.0 g of molecular

sieves (3Å) was added and the reaction mixture was refluxed for 1 h (Supplementary Figure S1B). On completion, the reaction mixture was filtered and solvent was evaporated *in vacuo*. The residue was purified through column chromatography over silica gel (60–120 mesh), eluted with chloroform-acetone (99:1), and recrystallized from hexane-chloroform to get benzimidazole 34 as creamy amorphous powder in 89% yield.

Yield = 89%; creamy-amorphous powder; M.P. = 233–235°C; ¹H NMR (CD₃OD, 500 MHz): δ7.19–7.22 (m, 4H, 4xCH, aromatic), 7.58–7.56 (d, 2H, 2xCH, aromatic), 8.04–8.06 (m, 2H, 2xCH, aromatic); ¹³C NMR (CD₃OD, 125 MHz): δ117.08, 117.25, 124.08, 127.58, 130.10, 130.16, 152.53, 164.47, 166.46; ESI-TOF HRMS (MeOH): m/z [M+H]⁺ calculated for C₁₃H₁₀FN₂, 213.0828, found 213.0823. Physical data of the rest of the compounds were recently reported (Chaturvedi et al., 2018).

Drugs

U46619 (a thromboxane analogue), acetylcholine (acetylcholine chloride; ACh), dimethylsulfoxide (DMSO), 1H-[1,2,4]oxadiazolo [4,3-a]quinoxalin-1-one (ODQ), trichloroacetic acid (TCA), calcium chloride (CaCl₂), EGTA, Bay K8644, tetraethyl ammonium (TEA), iberiotoxin, 4-aminopyridine (4-AP), glibenclamide, angiotensin II, smooth muscle α-actin antibody, TRITC-phalloidin, and 4',6'-diamidino-2-phenyl indole (DAPI) were obtained from Sigma-Aldrich (St Louis, MO-United States). Papain (EC number: 3.4.22.2), collagenase (EC number: 3.4.24.3), trypsin (EC number: 3.4.21.4), and DMEM were purchased from Sigma Chemicals, India Limited. All other chemicals and salts were purchased from E-Merck India Limited and Sigma Chemicals, India Limited. A cGMP (cyclic guanosine monophosphate) ELISA kit was obtained from Cayman Chemical (Anna Abor, MI, United States). Fetal Bovine Serum (FBS), a FluxOR™ II Green Potassium Ion Channel Assay kit, and Fluo-4 NW Calcium Assay Kits were obtained from Invitrogen (Paisley, United Kingdom). The stock solutions of the molecules studied were prepared in DMSO and were further diluted in bath fluids. The final concentration of DMSO did not exceed 0.1% in the bath solution.

Animals

All animal care and experiments were carried out following the Institutional Animal Ethics Committee (IAEC) approved protocols (CIMAP/IAEC/2016(07)-2019/33, CIMAP/IAEC/2016-2019/01 for hypertension and toxicity studies, respectively) followed by recommendations of the Committee

for the Purpose of Control and Supervision of Experiments on Animals (CPCSEA), Government of India. All the animals were maintained with an automated dark/light cycle of 12 h with controlled temperature ($22 \pm 5^\circ\text{C}$) and humidity ($45 \pm 5\%$). The animals were fed with the standard rat feed and were provided with drinking water *ad libitum*. Prior to the actual experiments, all the animals were acclimatized for 7 days in the experimental environment. For the *ex vivo* and *in vitro* studies, male and female Wistar rats of 180–250 g were used, while male spontaneously hypertensive rats (SHRs) were used to assess *in vivo* antihypertensive activity. Male and female Swiss albino mice were used in acute and sub-acute oral toxicity tests.

Tissue Preparation for *Ex Vivo* Vasorelaxation Study

Wistar rats weighing 180–250 g were sacrificed under anesthetized conditions using ketamine (80 mg kg^{-1}) and xylazine (10 mg kg^{-1}). The intestine was excised and placed in aerated cold modified Krebs-Henseleit solution (MKHS) containing 118 mM of NaCl; 24 mM of NaHCO_3 ; 4 mM of KCl; 1.8 mM of CaCl_2 ; 1 mM of MgSO_4 ; 0.43 mM of NaH_2PO_4 ; and 5.56 mM of glucose. The superior mesenteric artery was dissected and cleaned from the surrounding adipose tissue, and cut into rings of 2–3 mm in length. These rings were mounted in a dual-chamber small-vessel wire myograph (Danish Myo Technology, Aarhus, Denmark) containing 5 ml of MKHS maintained at 37°C with continuous bubbling in carbogen gas (95% oxygen and 5% carbon dioxide). The tissue was stretched to the basal tension of 5–6 mN and equilibrated for 60 min with continuous change in buffer at every 15 min. The tissue viability was assessed by high potassium depolarizing solution (80 mM) evoked contraction, and endothelium integrity was confirmed by ACh relaxation response over U46619 (100 nM)-induced contraction and was used for the assessment of vasorelaxation response of benzimidazole analogues (Singh et al., 2019).

In vivo Antihypertensive Activity in SHRs

Six to eight-week-old male SHRs weighing 200–250 g were taken for the study. FPD was solubilized in groundnut oil and was administered orally to SHRs at a dose of 50 mg kg^{-1} and 100 mg kg^{-1} while the vehicle control group received only groundnut oil. A known antihypertensive drug, minoxidil (a potassium channel opener), was dissolved in water and was given orally at a dose of 10 mg kg^{-1} . All the animals were subjected to the treatment for 14 days. After 14 days, the hemodynamic parameters and heart rate of all the animals was studied using an invasive blood pressure method. Invasive blood pressure measurement was done by anesthetizing the animal with ketamine (80 mg kg^{-1}) and xylazine (10 mg kg^{-1}). The carotid artery was exposed, a non-occlusive polyvinyl catheter (PE catheter) was inserted, and blood pressure was measured using an analog-to-digital interface (PowerLab Data acquisition

system, ADInstruments Inc., Australia). The data were analyzed by LabChart software V 8.0.

Elucidation of Mechanisms of Vasorelaxation: Ion Channels and Pathways

To elucidate the role of the endothelium in the relaxation response, vascular reactivity was studied in both intact and denuded endothelium rings. Denudation of the endothelium was done mechanically by rubbing the lumen of blood vessels with human hair and was confirmed by loss of relaxation response to acetylcholine ($10 \mu\text{M}$) to less than 10%. Since, most of the antihypertensive benzimidazoles are known to act via blockade of the AT1 receptor, we checked the most potent molecule FPD (c-substituted fluorophenyl benzimidazole) for AT1 receptor blocking activity by pre-exposing mesenteric arterial rings to FPD ($10 \mu\text{M}$) for 20 min followed by elicitation of contraction response to Ang II ($1 \mu\text{M}$) (Jain et al., 2020).

The contribution of potassium channels in the relaxation response was explored by eliciting contraction response with both 80 mM of high K^+ MKHS (containing 42.7 mM of NaCl; 24 mM of NaHCO_3 ; 80 mM of KCl; 1.8 mM of CaCl_2 ; 1 mM of MgSO_4 ; 0.43 mM of NaH_2PO_4 ; and 5.56 mM of glucose) and a low potassium depolarizing solution (25 mM of high K^+ MKHS containing 97.7 mM of NaCl; 24 mM of NaHCO_3 ; 25 mM of KCl; 1.8 mM of CaCl_2 ; 1 mM of MgSO_4 ; 0.43 mM of NaH_2PO_4 ; and 5.56 mM of glucose), prepared by equimolar replacement of NaCl with KCl in MKHS. The cumulative concentration-response to FPD was studied. Further, to identify the involvement of potassium channel subtypes in the relaxation response of FPD, superior mesenteric arterial rings were pretreated with blockers of BK_{Ca} channel, TEA (1 mM) or iberiotoxin (10 nM); K_{ir} channel (BaCl_2 , $30 \mu\text{M}$); K_{V} channel (4-AP, $300 \mu\text{M}$) and K_{ATP} channel (glibenclamide, $10 \mu\text{M}$), and the relaxation response to FPD was elicited in a concentration-dependent manner in agonist pre-constricted arterial rings. U46619 (100 nM) was used as an agonist for inducing contraction for all the potassium channel subtype blockers except glibenclamide where noradrenalin ($10 \mu\text{M}$) was used as an agonist for pre-incubation because glibenclamide markedly inhibits contraction response to U46619 (Chanda et al., 2016).

To evaluate the role of the sGC-cGMP-PKG pathway, the arterial rings were incubated in ODQ ($10 \mu\text{M}$, a sGC inhibitor) for 20 min and the relaxation response was studied. In another set of experiments, the role of VDCC in FPD-induced vasorelaxation was investigated. Briefly, after checking the tissue viability and endothelium integrity, the involvement of VDCC in FPD-induced relaxation was assessed by a developing concentration-dependent contraction response to Bay K8644 (a known opener of L-type VDCC) in slightly depolarized (High K^+ , 15 mM) tissues in the presence and absence of FPD (Alonso et al., 1989).

Measurement of Intracellular cGMP Level

Endothelium-intact rat superior mesenteric artery segments of approximately 5 mg in weight were prepared and kept under

physiological conditions in 1 ml of MKHS at 37°C and were aerated continuously with carbogen gas throughout the experimental procedure. After 30 min of equilibration, treatment with compounds was given as follows.

- Vehicle control, DMSO (3 μ l for 10 min).
- FPD (10 μ M for 20 min).
- FPD (30 μ M for 20 min).
- U46619 (100 nM for 10 min).
- U46619 (100 nM for 10 min) followed by FPD (10 μ M for 20 min).
- SNP (1 μ M for 20 min).

Treated tissues were immediately frozen with liquid nitrogen and were pulverized in pre-chilled pestle and mortar. Two hundred microliters of 5% TCA was added and the samples were homogenized. These samples were centrifuged at 1,500 g for 10 min at 4°C. The obtained supernatant was made free of TCA by extraction with water saturated ether five times, and at the end the residual ether was removed by heating the supernatant at 70°C for 15 min and was used as a source of cGMP. The ELISA was performed using the manufacturer's guidelines (Cayman Chemical Company, Ann Arbor, United States). Remaining tissue pellet was used for the estimation of protein concentration. For this, the pellet was dissolved in 100 μ l of 0.1 N NaOH and the concentration of protein in the pellet was determined using a Pierce™ BCA Protein Assay kit (Thermo Scientific, Rockford, United States) and the level of cGMP was expressed as pmol mg⁻¹ protein (Singh et al., 2017).

***In vitro* Assessment of FPD-Induced Modulation of Potassium and Calcium Channel Functions in VSMCs**

Isolation of Primary Rat Vascular Smooth Muscle Cells

The aorta of Wistar rats were aseptically isolated and cleaned of adhering fatty and connective tissue in the presence of 1% antibiotic solution in MKHS. The tissue was washed, chopped, and digested in an enzymatic mixture of papain (1 mg ml⁻¹), collagenase (2 mg ml⁻¹), and dithiothriitol (1 μ M) in HEPES buffer for 30 min at 37°C in water bath. Over the incubation period, the mixture was shaken repeatedly every 10 min. The digested tissue sample was washed three times with HEPES buffer, suspended in DMEM supplemented with 10% FBS. The single cell suspension was seeded in a 25 cm² cell culture flask and was incubated in 5% CO₂ at 37°C. Rat aortic VSMCs were allowed to grow at 37°C in a 5% CO₂ incubator. The cells were maintained in DMEM supplemented with 10% FBS, and the medium was replaced twice a week. VSMCs between passages 5 and 9 were used in all the experiments (Prieto-Lloret et al., 2018).

Immunocytochemistry of Rat VSMCs

To exemplify and evaluate the purity of the obtained cell populations, immunocytochemistry of rat aortic VSMC was performed following the methodology published earlier (Weber et al., 2011). Briefly, the aortic cell suspension was plated onto the chamber slide and was allowed to attach. The cells were then fixed by 4% paraformaldehyde and 4% polyethylene glycol 600 with 3 mM of EGTA and 2 mM of MgCl₂ in PBS. Cells were permeabilized with 0.1% Triton

X-100 and were washed three times with PBS. The cells were blocked with 5% skimmed milk for 30 min and then were treated with a smooth muscle α -actin antibody (1:500 in 5% skimmed milk) for 60 min. After being washed twice with PBS, the cells were incubated in goat anti mouse IgG (H + L) and DyLight™ 488 conjugated secondary antibody (1:2,000 in 5% skimmed milk) for 60 min in dark. For the visualization of F-actin, the cells were incubated with 0.5 μ M of TRITC-phalloidin for 20 min at room temperature. The cell nucleus was stained with DAPI, washed and mounted in the mowiol mounting medium. Cells were examined using a ZEISS Confocal laser scanning microscope (LSM 880 Carl Zeiss microscopy, Germany).

Potassium Channel Function Assay in VSMCs

To explore the effect of FPD on potassium channel opening, a FluxOR™ II Green Potassium Ion Channel Assay (Invitrogen, Paisley, United Kingdom) was carried out in VSMCs following the manufacturer's guidelines. In brief, rat aortic smooth muscle cells were resuspended in the growth medium and were plated at 2×10^3 cells per well in a 96-well plate. Cells were allowed to adhere overnight at 37°C. When the cells were attached, growth medium was replaced by the 1X loading buffer. Cells were incubated at 37°C for 60 min to facilitate dye entry. Further loading buffer was removed and assay buffer was added in each well. Treatment with 10 μ M of FPD, 30 μ M of FPD, 10 mM of TEA, and 80 mM of KCl were given for 20 min in different wells, and the FluxOR II assay was performed using Spectramax i3 (Molecular Devices, United States). The instrument was set at the excitation wavelength of 480 nm and the emission wavelength of 535 nm. Initially, 50 baseline readings were taken and after that 2 mM of thalium ion solution was injected and the fluorescence was studied for 5 min at every 0.4 s. The data were presented in the form of area under curve and a line diagram was plotted as relative fluorescence unit vs. time in seconds.

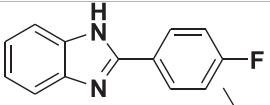
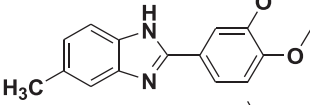
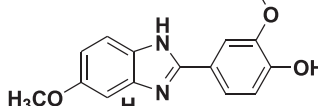
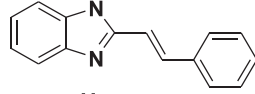
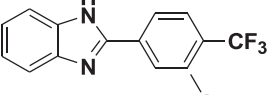
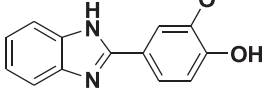
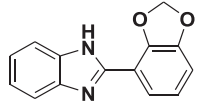
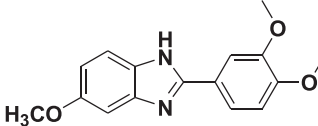
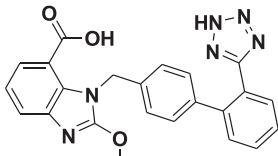
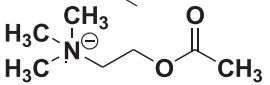
Calcium Imaging

Rat aortic smooth muscle cells were plated at about 30,000 cells per well in a 96-well plate in DMEM with 10% FBS and was left overnight to reach confluency. The rest of the procedure was done according to the manufacturer's recommendations (Fluo-4 NW Calcium Assay Kit, Invitrogen, Paisley, United Kingdom). Growth medium was removed from the adherent cell cultures and the dye loading solution was added to each well. Cells were allowed to load the dye for 30 min at 37°C. The cells were then exposed to treatment with 10 and 30 μ M of FPD for 20 min. Initial baseline fluorescence was measured and thereafter either NE (10 μ M) or Bay K8644 (1 μ M) was injected both in the presence and absence of FPD and the change in the relative fluorescence was studied to quantify the intracellular calcium concentration. The data were presented in the form of area under curve and line diagram.

In silico Docking Study

To complement the pharmacological observations, the docking studies were done with the identified protein targets. Based on the *ex vivo* observations, we chose angiotensin II receptor 1 (AT1), sGC, BK_{Ca} channels, and L-type VDCC as target proteins and FPD

TABLE 1 | Screening of novel benzimidazole class of compounds for vasorelaxation in isolated endothelium-intact rat superior mesenteric arterial rings against U46619 (100 nM)-induced contraction. Acetylcholine (10 μ M)-induced relaxation is considered as positive control for the screening (mean \pm SEM, $n = 5$).

Compound (10 μ M)	Structure of compound	Percent relaxation
1 FPD		97.8 \pm 0.7
2 MPD		90.7 \pm 3.3
3 AMPD1		75.7 \pm 4.9
4 TCPD		46.2 \pm 5.1
5 CFPD		43.4 \pm 5.7
6 VPD		54.3 \pm 6.1
7 23PD		37.1 \pm 4.6
8 MOPD		31.2 \pm 6.2
9 Candesartan		80.6 \pm 6.5
10 Acetylcholine		95.5 \pm 0.7

as a candidate molecule. Along with this, we took Bay 41-2,272 (Pubchem CID: 9798973) for sGC; tetraethylammonium chloride (Pubchem CID: 5946) for BK_{Ca} channel, nifedipine (Pubchem CID: 4485) for VDCC, and candesartan (Pubchem CID: 2541) for AT1 receptor as standards for the docking experiment.

Homology Modeling

Prior to the docking studies, the mining of the PDB structure of all the targets was carried out and the crystal structures of BK_{Ca} channels (PDB ID: 3NAF), VDCC (PDB ID: 1T0H), and

angiotensin II receptor 1 (PDB ID: 4YAY) were considered for docking. Since suitable crystal structures of the target sGC β subunit could not be identified in the protein database, we created the homology model using the SWISS-MODEL Workspace webserver (Alam et al., 2020). The amino acid sequence of sGC (Organism: *Rattus norvegicus*) with the prescribed length was retrieved from the UniProtKB database (P20595). To identify a suitable template protein 3D structure for modeling, we searched the PDB database by BLAST. The model was built based on template protein for human guanylate cyclase soluble subunit beta-1 (PDB ID: 6JT0). The homology 3D protein structure of this protein described as homology model_1 is represented in **Supplementary Figure S3**.

Protein Preparation and Docking With Ligands

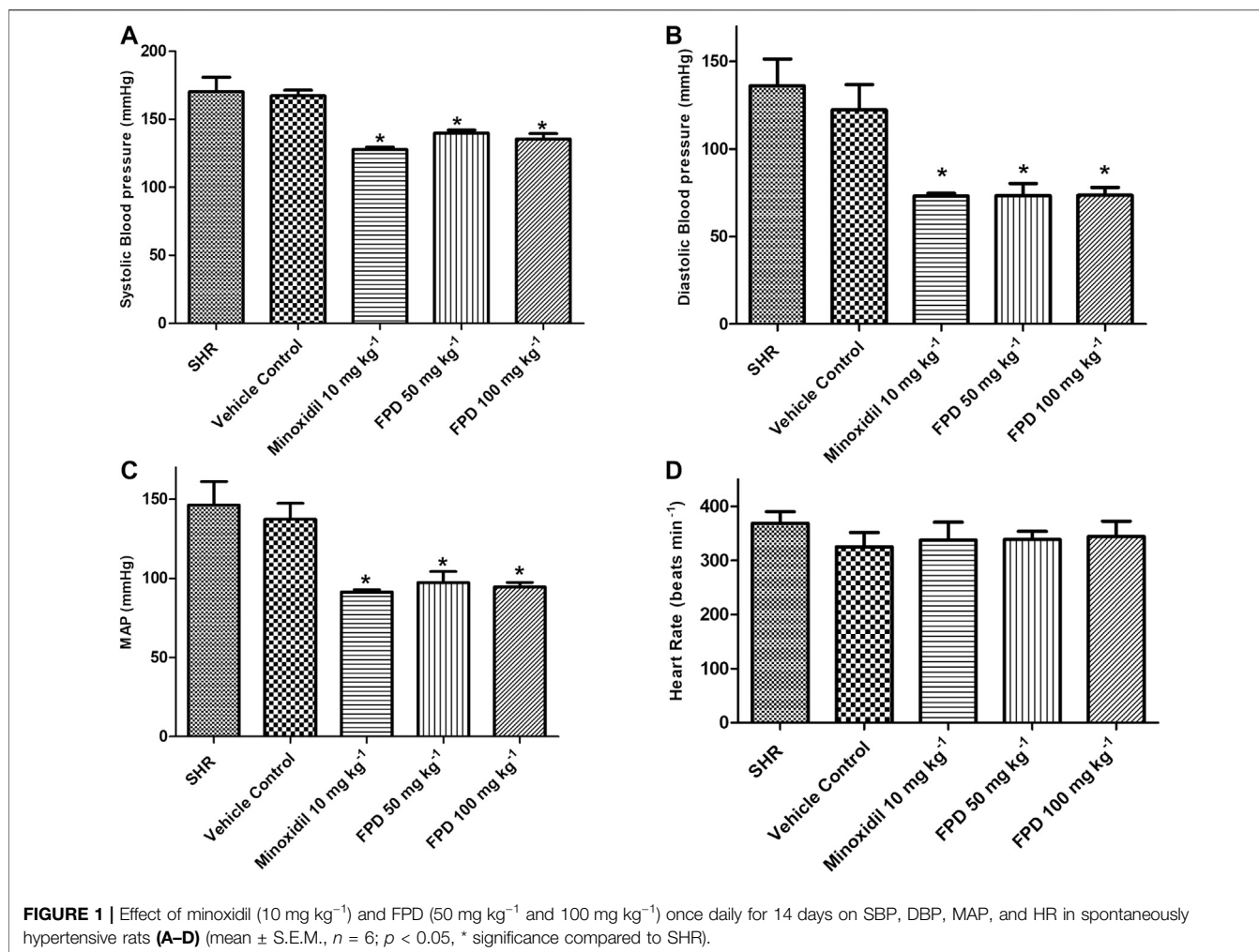
The protein preparation protocol of Discovery Studio was used to perform tasks such as inserting missing atoms in incomplete residues, deleting alternate conformations (disorder), removing waters, standardizing the names of the atoms, modeling missing loop regions, and protonating titratable residues using predicted pKs (negative logarithmic measure of the acid dissociation constant). CHARMM (Chemistry at HARvard Macromolecular Mechanics; Cambridge, MA, United States) was used for protein preparation. Hydrogen atoms were added before the processing. Protein coordinates from the crystal structure of the targets were considered for the docking experiment (Alam and Khan, 2018). For the docking and visualization studies, the LibDock program of Discovery Studio version 3.5 (Accelrys, United States, 2013) was used (Alam and Khan, 2019) where protein site features were referred to as hot spots and were of two types (polar and non-polar). The ligand poses were then placed into this polar and non-polar receptor interactions site. For energy minimization, the SMART minimizer algorithm was used. The CHARMM force field was used in the parameterization step. The best conformation of each ligand was selected according to their position in the active site and the docking score. Selected conformations were used for the analysis of interactions with residues of the active site of the targets (Das et al., 2020).

Toxicity

Acute and sub-acute oral toxicity was carried out following previously published protocol (Chanda et al., 2009; Singh et al., 2019). Swiss albino mice were treated with FPD at 5, 50, 300, and 1,000 mg kg⁻¹ once orally in the acute oral toxicity test and at 0.1, 1, 10, and 100 mg kg⁻¹ once daily by oral route for 28 days in sub-acute oral toxicity test. The animals were kept under observation during the course of experiment for any sign of illness, mortality, morbidity, and change in way of walking and posture. Body weight was taken, hematology, serum biochemistry, gross observation of vital organs, and their absolute and relative weights were recorded at the end of the acute and sub-acute toxicity experiments.

Statistical Analysis

Relaxation responses of the benzimidazole analogues were expressed as the percent reversal of the U46619 or high K⁺



MKHS-induced contraction of the rat mesenteric arterial rings. Concentration-response curves were fitted to sigmoidal curves by nonlinear regression analysis (log agonist vs. normalized response, with variable slope), using Graph Pad Prism version 5.00 (San Diego, California, United States) to calculate the pD₂ values (log molar concentration of the agonist producing 50% of the maximal response). Concentration-response curves were analyzed with repeated measures two-way ANOVA (treatment vs. concentration), and Bonferroni post tests were used to compare replicate means. The E_{max}, AUC values, and *in vivo* comparisons between control and treated groups were made using one-way ANOVA with post hoc analysis using Tukey's multiple comparison test or *t* test, as appropriate. AUC was also calculated by the GraphPad software. A value of *p* < 0.05 was considered statistically significant. Column statistics were used to calculate mean and standard error and the results were expressed as mean ± standard error of the mean (SEM), with *n* equal to the number of arterial rings from different animals (biological replicates) or independent experiments.

RESULTS

Synthesis of Benzimidazole Analogues

The synthesis protocol is depicted in **Supplementary Figure S1B**. *O*-phenylenediamine was condensed with various benzaldehydes in the presence of 3Å molecular sieves. Two series of products were obtained on the benzimidazole core, *i.e.*, 2-arylbenzimidazoles (33–48) in 30–89% as major products and 1, 2-diarylbenzimidazoles (49–53) as a minor product (<8%) (Chaturvedi et al., 2018).

Novel Benzimidazole as Vasodilator in Superior Rat Mesenteric Arteries

All the compounds chosen for the study relaxed the U46199 (100 nM) pre-contracted rat superior mesenteric artery at 10 μM considering acetylcholine-induced (10 μM) vasorelaxation as standard (**Table 1**). A further three compounds showing E_{max} > 70% were chosen for the concentration-dependent relaxation (**Supplementary Figure S2**). Out of the molecules studied, FPD

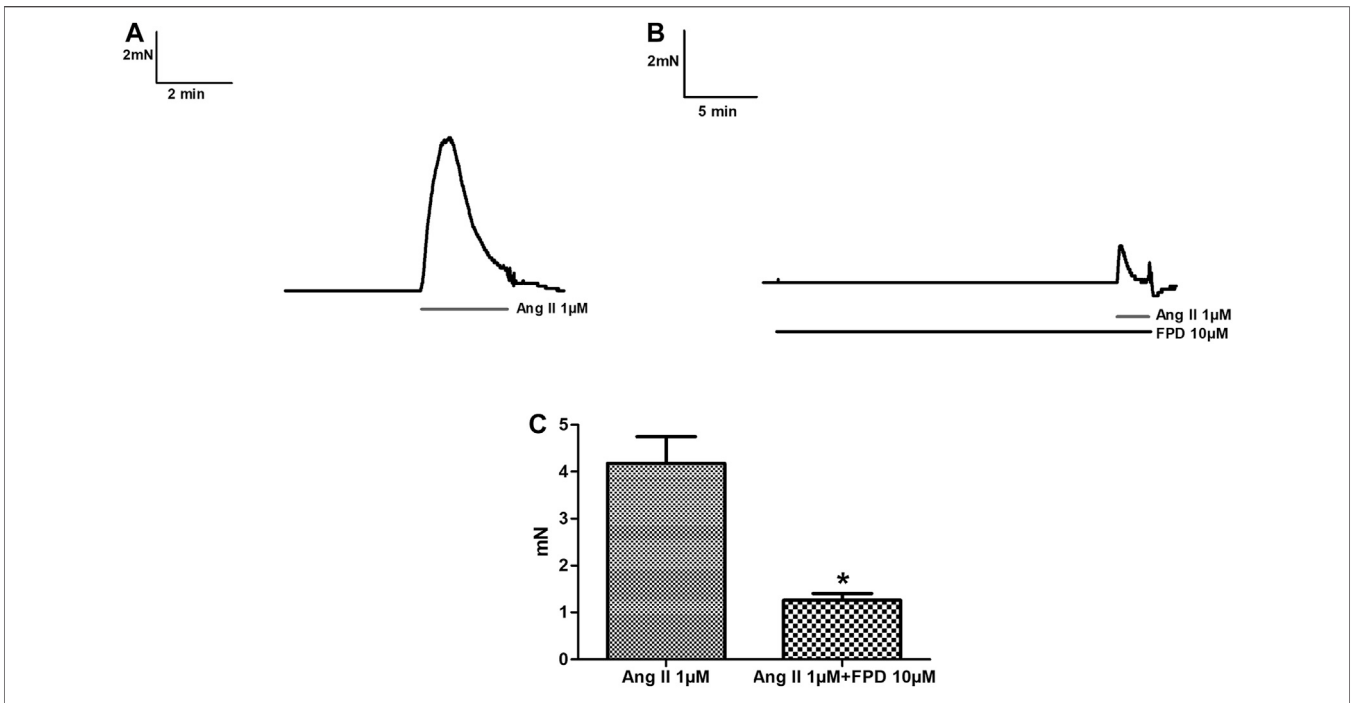


FIGURE 2 | Traces showing angiotensin II (1 μ M)-induced contraction in isolated rat superior mesenteric arterial rings **(A)** and in a pre-incubated arterial ring with FPD (10 μ M) **(B)**. Contraction is expressed as the mean \pm S.E.M. ($n = 6$); * $p < 0.05$ compared to control **(C)**.

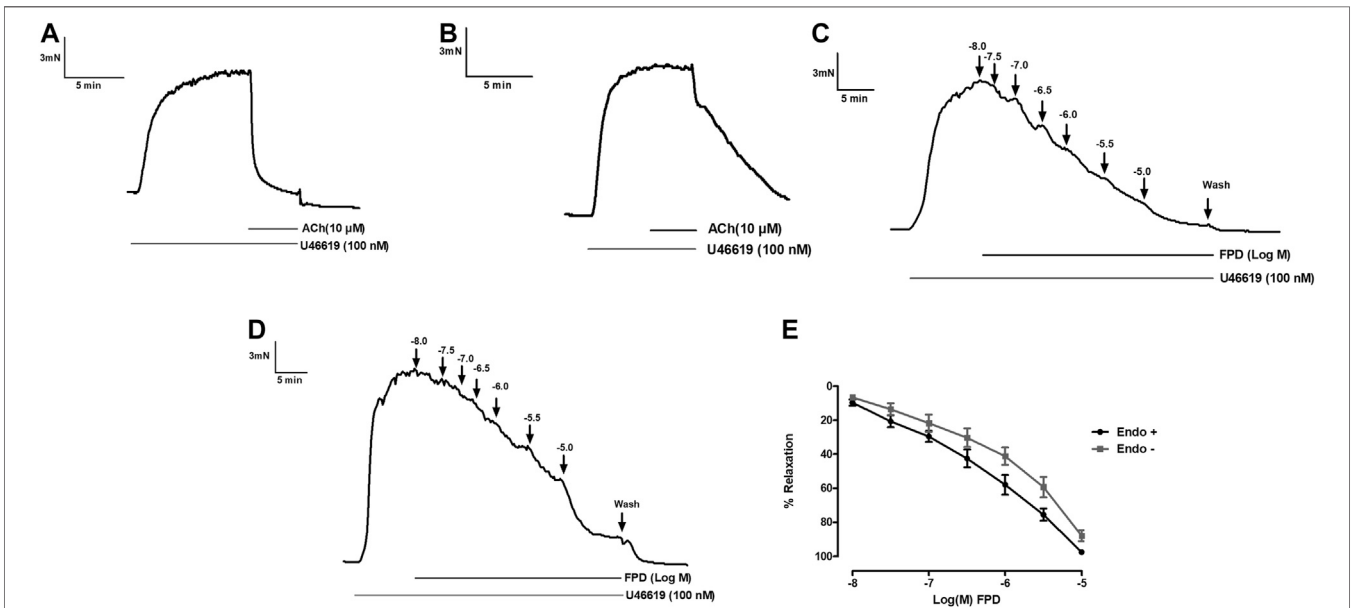
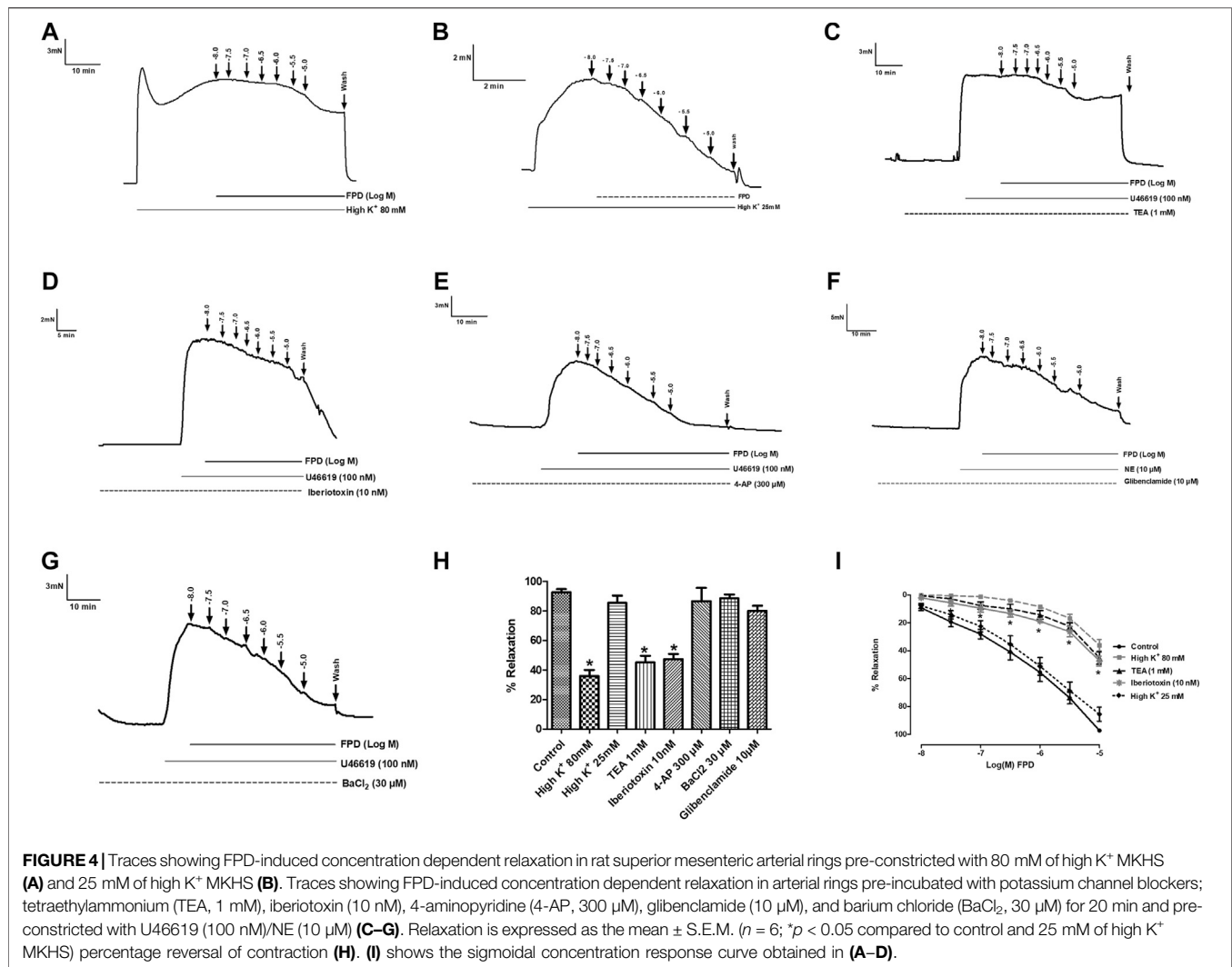


FIGURE 3 | Traces showing acetylcholine (10 μ M)-induced relaxation in endothelium-intact **(A)** and endothelium-denuded **(B)** isolated rat superior mesenteric arterial rings pre-constricted with U46619 (100 nM). Traces showing FPD-induced concentration dependent relaxation in endothelium-intact **(C)** and endothelium-denuded **(D)** arterial rings pre-constricted with U46619 (100 nM). E shows the sigmoidal concentration response curve obtained in **(C, D)**. Relaxation is expressed as the mean \pm S.E.M. ($n = 8$) percentage reversal of U46619-induced contraction.



produced the best concentration-dependent relaxation response and was taken for the detailed study (Supplementary Figure S2).

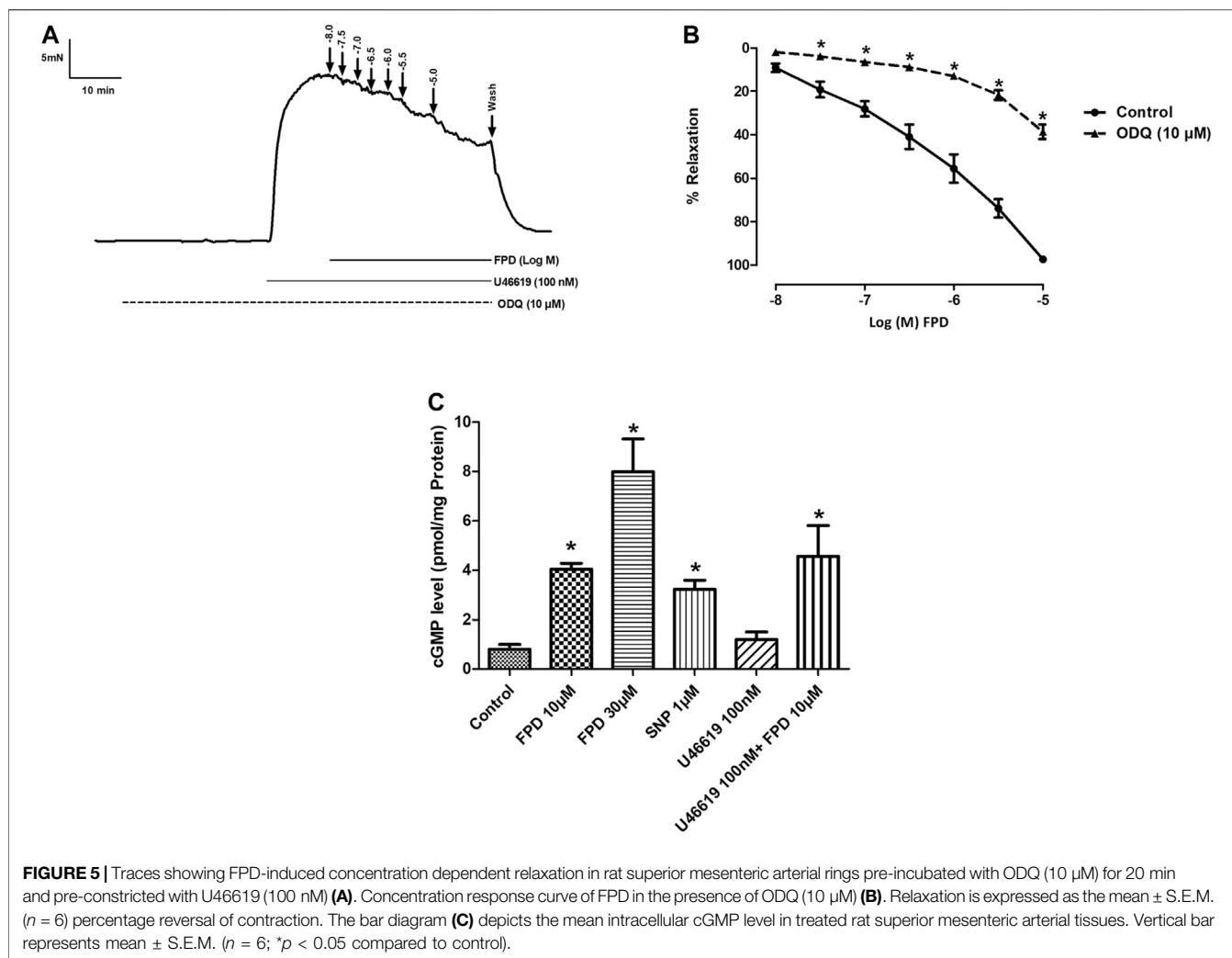
FPD Produced Potent Anti-hypertensive Activity in SHR

SHRs are one of the most commonly studied rodent models of hypertension for evaluating antihypertensive activity of pharmacophores in general and AT-1 receptor blockers from benzimidazoles like candesartan and telmesartan (Rizzoni et al., 1998; Cheng et al., 2018). In the present study, the novel fluorophenyl benzimidazole (FPD) was evaluated for *in vivo* antihypertensive activity in SHRs. Oral administration of FPD at 50 and 100 mg kg⁻¹ for 14 days showed a significant decrease in SBP, DBP, and MAP as compared to vehicle control SHRs and are presented in Figure 1. Minoxidil (10 mg kg⁻¹)-treated SHRs also showed a significant decline in hemodynamic parameters when compared with the control SHRs. The heart rate of treated rats remained unaffected compared to control (Figure 1D).

Role of AT₁ Receptor, cGMP Buildup, and Opening of BK_{Ca} Channel in FPD-Induced Vasorelaxation

Benzimidazoles as a class are known to produce antihypertensive activity through blockade of the AT₁ receptor. In the present study, the AT₁ receptor blocking potential of FPD was evaluated with angiotensin II-induced contraction pre-incubated with or without FPD and a significant blockade to angiotensin II-induced contraction was observed (Figure 2).

To study the role of the endothelium, the vasodilation response of FPD was evaluated using endothelium-intact and -denuded mesenteric arterial rings. Endothelium-denuded arterial rings produced no or less than 10% relaxation response to acetylcholine (10 μM) (Figures 3A,B). The concentration-dependent relaxation response to FPD in both endothelium-intact and -denuded rings showed no statistical difference in E_{max} (95.7 ± 1.2%; n = 12 for endothelium-intact and 88.9 ± 4.9%; n = 8 for endothelium-denuded mesenteric arterial rings) and pD₂ (6.3 ± 0.1; n = 12 for endothelium-intact



and 5.8 ± 0.1 ; $n = 8$ for endothelium-denuded mesenteric arterial rings) values (Figures 3C–E) suggesting endothelium-independent relaxation in the rat superior mesenteric artery. There are only a few reports on the modulation of potassium channel function by benzimidazoles (Lloyd et al., 2009) and no report is available on fluorobenzimidazole. Interestingly, when the superior mesenteric arterial rings were exposed to 80 mM of high K^+ MKHS to prevent potassium channel-mediated hyperpolarization, the relaxation response to FPD was significantly diminished, but a contraction response with a lower concentration of K^+ (25 mM of KCl containing MKHS) showed a complete concentration-dependent relaxation response to FPD suggesting an opening of potassium channels (Figures 4A,B). The involvement of sub-types of K^+ channels in FPD-induced relaxation was studied in agonist (U46619/norepinephrine)-constricted arterial rings and is presented in Figures 4C–G. The results showed that pre-incubation of arterial rings with either TEA (1 mM) or iberiotoxin (10 nM) (Ca^{2+} -activated K^+ channel blocker; BK_{Ca} channel) abolished the relaxation response significantly

in E_{max} ($95.7 \pm 1.2\%$; $n = 12$ for control to $45.3 \pm 5.4\%$; $n = 6$ for 1 mM of TEA and $47.4 \pm 3.5\%$; $n = 6$ for 10 nM of iberiotoxin treated mesenteric rings) and pD2 (6.3 ± 0.1 ; $n = 12$ for control to 4.8 ± 0.1 ; $n = 6$ for 1 mM of TEA and 4.8 ± 0.1 ; $n = 6$ for 10 nM of iberiotoxin treated mesenteric rings) values and are presented in Figures 4H,I.

The involvement of the sGC-cGMP-PKG pathway was also studied in the vasodilation response of FPD in the superior mesenteric artery. Pre-incubation of mesenteric arterial rings with ODQ for 20 min significantly abated the effect of FPD with a decrease in E_{max} (from $95.7 \pm 1.2\%$; $n = 12$ for control to $38.6 \pm 3.3\%$; $n = 12$ for 10 μM of ODQ treated mesenteric rings) and pD2 (6.3 ± 0.1 ; $n = 12$ for control and 4.6 ± 0.1 ; $n = 12$ for 10 μM of ODQ treated mesenteric rings) values (Figures 5A,B). Further, FPD treatment of the arterial tissues showed a concentration-dependent increase in tissue cGMP level 5.05 fold at 10 μM and 9.97 fold at 30 μM compared to control in the cGMP ELISA assay. SNP (1 μM) also increased the cGMP level 4.03 fold compared to control (Figure 5C).

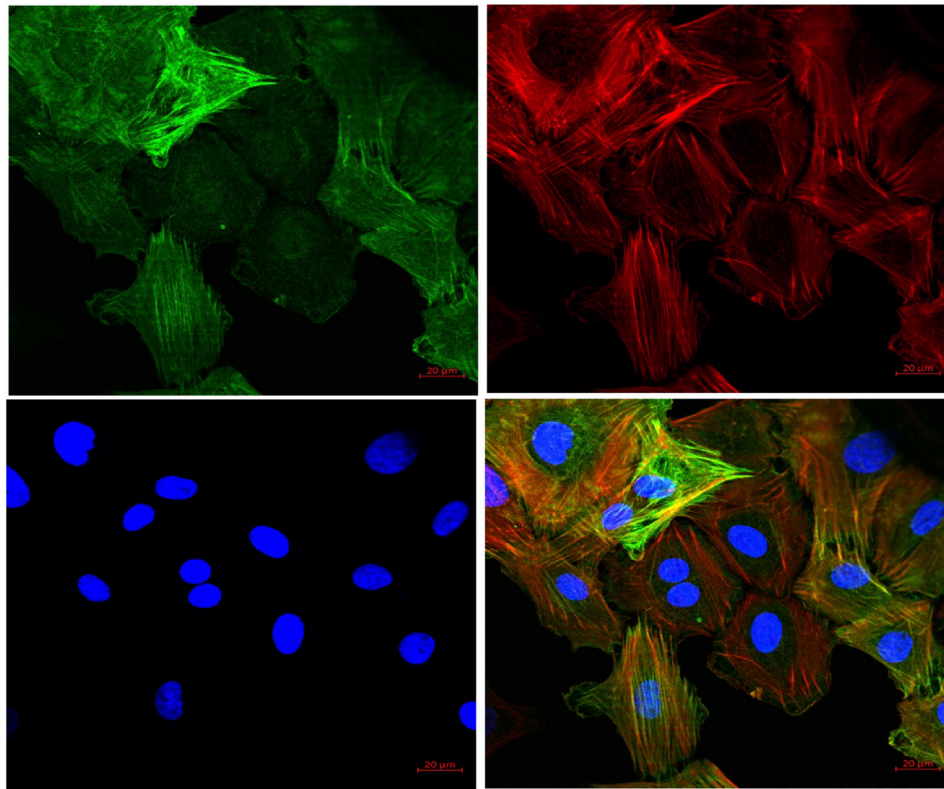


FIGURE 6 | Representative pictures of cells derived from rat aorta stained with markers for VSMCs. Mesenchymal marker alpha-smooth muscle actin (α -SMA) (green) and F-actin (red) were stained positive in VSMCs. The nucleus of VSMC was stained by DAPI (blue) (40X).

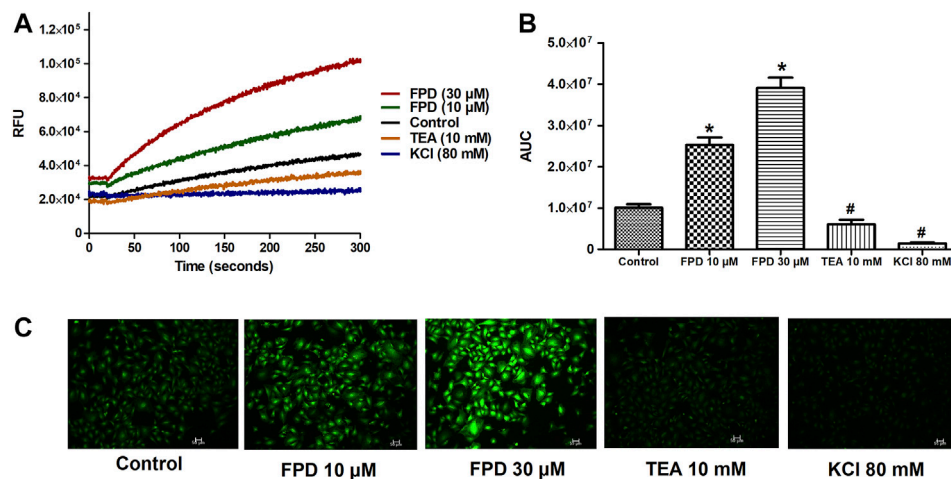
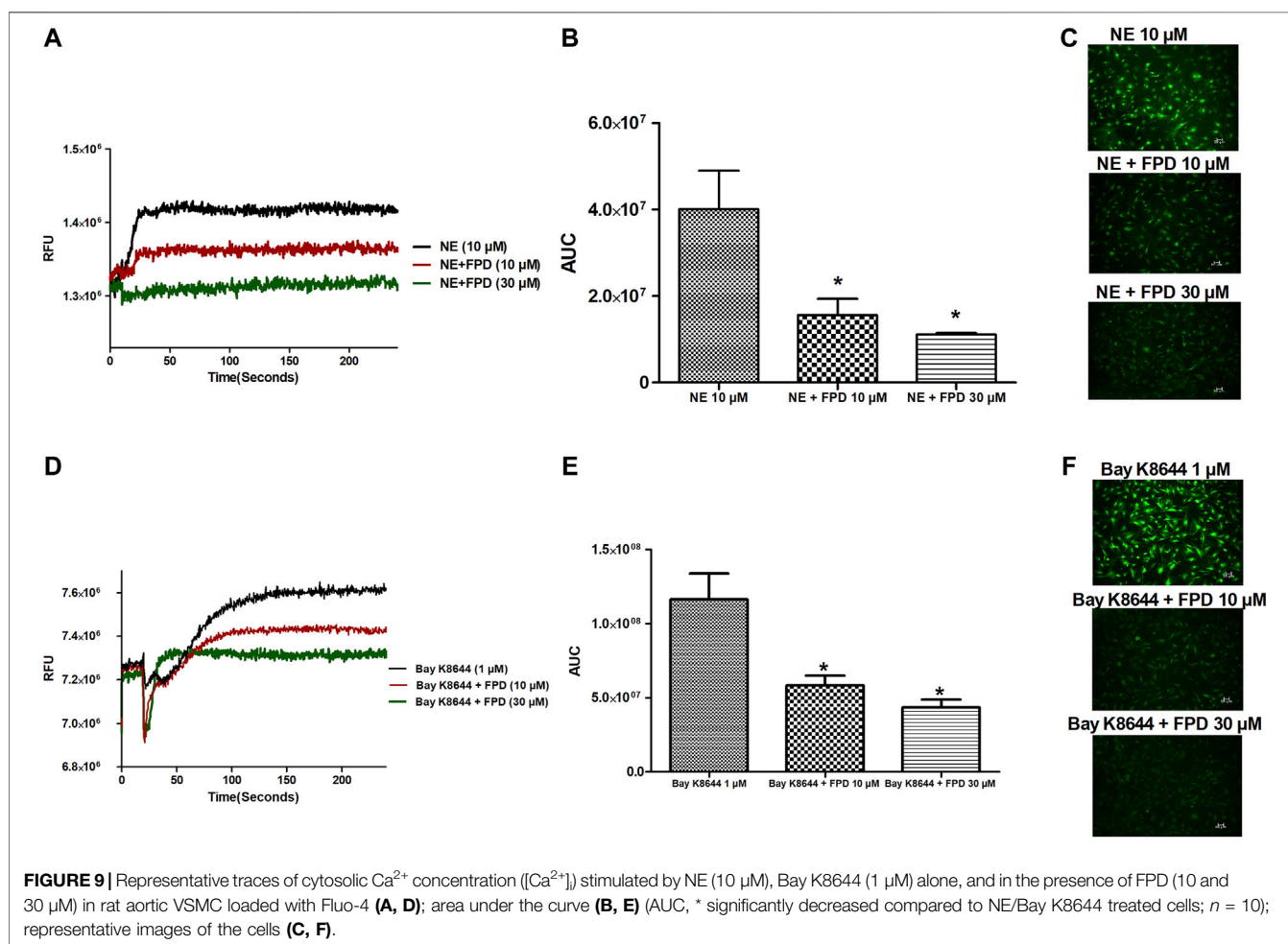
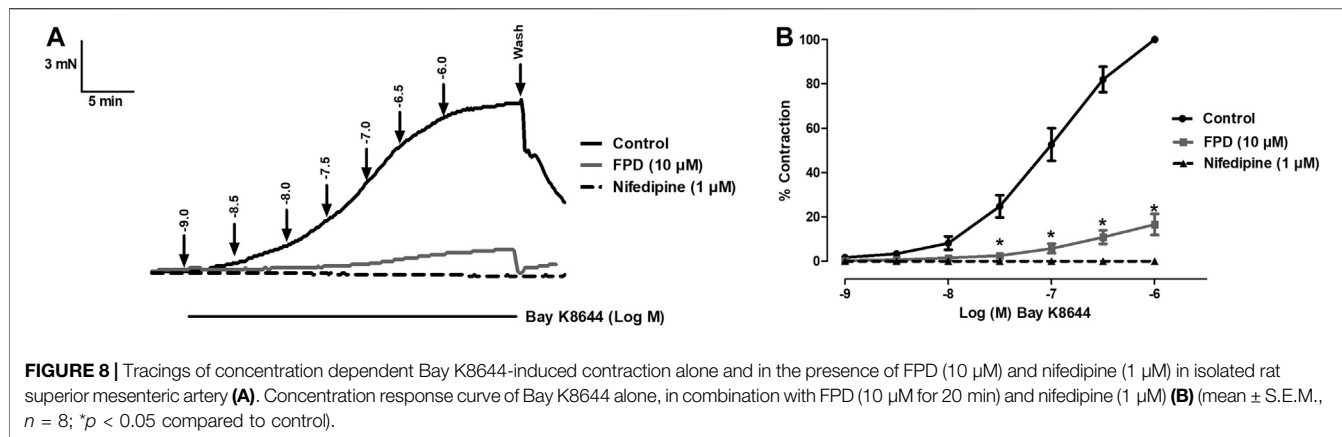


FIGURE 7 | Representative traces of intracellular K^+ concentration stimulated/inhibited by FPD (10 μ M), FPD (30 μ M), TEA (10 mM), and KCl (80 mM) in rat aortic VSMC loaded with FluxOR II Green **(A)**. **(B)** depicts the area under the curve (AUC); * significantly increased compared to control; # significantly decreased compared to control; $n = 10$. **C** shows the representative images of the cells.

FPD Enhanced Thallium Ion-Induced Fluorescence in Rat Aortic Smooth Muscle Cells

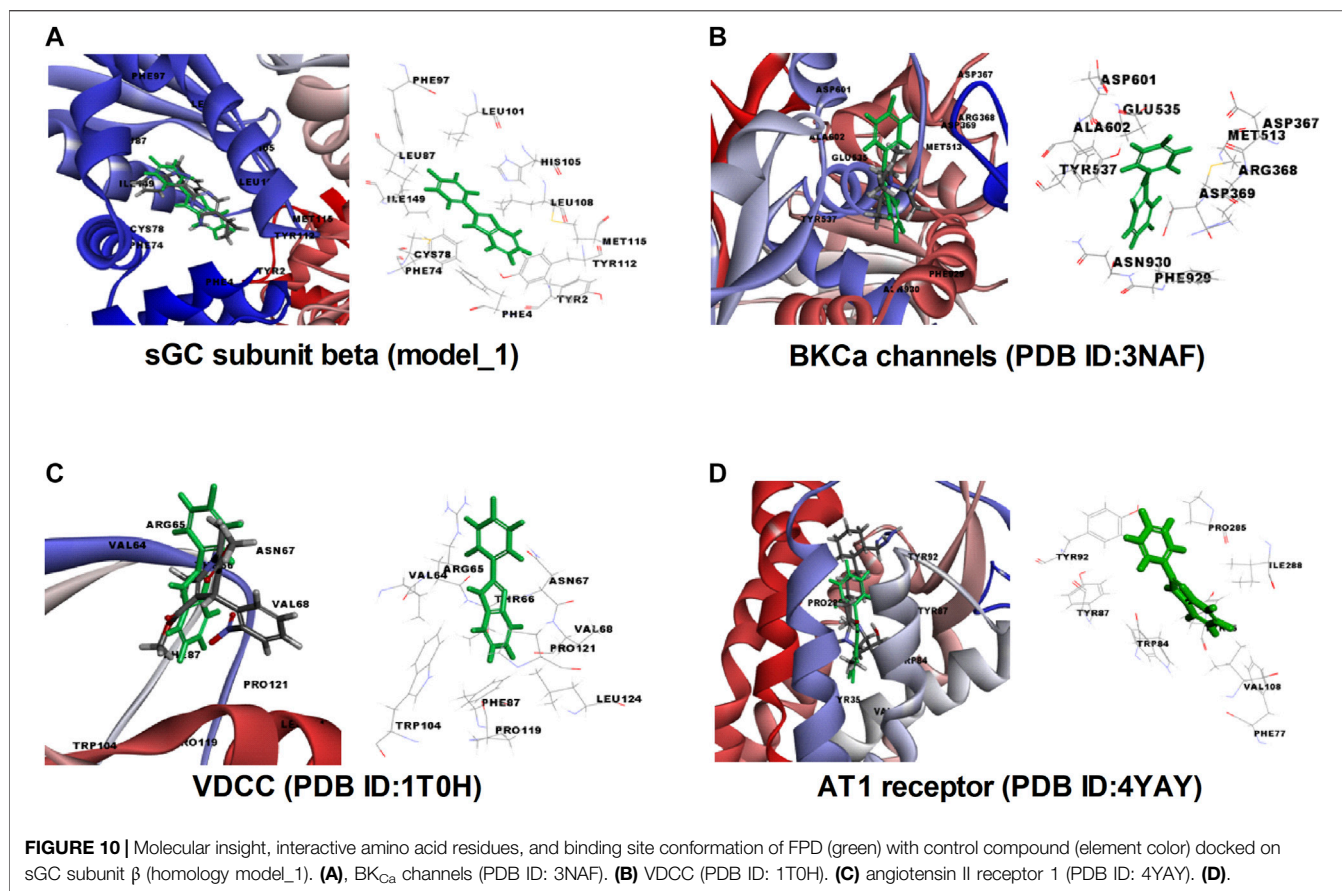
To further substantiate our *ex vivo* observations, an *in vitro* potassium channel function assay was performed in rat aortic

VSMC. Before conducting this assay, the characterization of VSMC was carried out using immunofluorescence staining and it was clearly seen that mesenchymal marker α -SMA and F-actin were stained positive (**Figure 6**). In the potassium



channel function assay, it was seen that cells pretreated with FPD at 10 and 30 μ M for 20 min showed a significant increase in relative fluorescence unit as compared to control, which clearly suggests that FPD led to the opening of the potassium channel, in which there is an

inward movement of thallium ions which binds to the cytosolic residing fluorescent dye and results in increased fluorescence. Moreover, the exposure of cells to 10 mM of TEA and 80 mM of KCl was found to significantly decrease the fluorescence (Figures 7A–C).



FPD Blocks Bay K8644-Sensitive VDCC in Rat Mesenteric Arteries and Reduces Intracellular Ca²⁺ Level in Rat Aortic Smooth Muscle Cells

As the relaxation response of FPD was not completely abolished either in the presence of high potassium depolarizing MKHS (~60%), TEA, or ODQ, the contribution of other targets like VDCC was explored to study the mechanism of vasorelaxation in the mesenteric artery. We used a specific L-type VDCC opener, Bay K8644, to study the involvement of VDCC in the vasodilation response of FPD in the superior mesenteric artery. Cumulative concentration-dependent contraction response of Bay K8644 from 1 nM to 1 μ M was elicited in slightly depolarized (K⁺, 15 mM) arterial rings (**Figure 8A**). Pre-incubation of arterial rings with FPD (10 μ M) or a known blocker of VDCC, nifedipine (1 μ M) independently for 20 min significantly abolished the contraction response induced by Bay K8644 (E_{\max} 100 \pm 0.0%; n = 8 control, 16.6 \pm 4.7%; n = 8 for FPD (10 μ M) and 0.0 \pm 0.0%, n = 5 for nifedipine (1 μ M) treated mesenteric rings) and pD₂ (7.1 \pm 0.0; n = 8 for control and 4.7 \pm 0.4; n = 8 for FPD (10 μ M) treated mesenteric rings) values (**Figures 8A,B**). To investigate the effect of FPD on intracellular Ca²⁺ level by inhibiting calcium channel function, a calcium fluorescence assay was carried out in the VSMC using Fluo-4 AM dye which strongly fluoresces when there is a rise in intracellular calcium concentration. In this experiment, we used NE (10 μ M) to induce VSMC [Ca²⁺]_i and it was found

that calcium elevation by NE (10 μ M) was significantly decreased in the FPD-treated cells at the concentration of 10 and 30 μ M, this is illustrated in **Figures 9A–C**. To further substantiate our finding that FPD blocks L-type VDCC; the cells were treated with Bay K8644 (1 μ M) and it was found that a rise of intracellular calcium concentration by Bay K8644 was significantly reduced in the FPD (10 and 30 μ M) pretreated cells (**Figures 9D–F**).

In silico Docking of FPD With AT₁, BK_{Ca} Channels, VDCC, and sGC

In order to validate our *ex vivo*, *in vitro*, and *in vivo* observation of potent vasorelaxation, cGMP buildup in arterial tissues, potassium and calcium channel function modulation, and antihypertensive activity with FPD, we docked our compound with selected target proteins, i.e., BK_{Ca} channels (PDB ID: 3NAF), VDCC (PDB ID: 1T0H), angiotensin II receptor 1 (PDB ID: 4YAY), and with a freshly modeled β subunit of sGC (model_1; **Supplementary Figure S3**). Docking of FPD with the selected targets resulted in a LibDock score of 63.87, 63.56, 60.55, and 69.15 for AT₁ receptor, BK_{Ca} channel, VDCC, and sGC β , respectively. The docking scores suggested that the compound had a fair chance of binding with all the selected protein targets. The results of the docking studies are summarized in **Figure 10** and **Table 2**. The analysis of the protein-ligand complexes

TABLE 2 | LibDock scoring functions, hydrogen bonding, Pi-interaction, and active binding site residues observed in the *in silico* docking studies of FPD with selected targets: sGC subunit beta (homology model_1), BK_{Ca} channels (PDB ID:3NAF), VDCC (PDB ID:1T0H), and angiotensin II receptor 1 (PDB ID:4YAY) using reported target specific ligands as a standard compound.

Target	PDB ID/ homology model	Ligands FPD/control	LibDock score	-H Bonding	Pi- interaction	Amino acid residues
sGC subunit beta	Model_1	FPD	69.15	No	PHE4 PHE74	TYR2, PHE4, PHE74, CYS78, LEU87, PHE97, LEU101, HIS105, LEU108, TYR112, MET115, ILE149
		CID:9798973 (Bay 41–2,272)	123.36	No	No	TYR2, PHE4, VAL5, PHE74, PHE75, CYS78, LEU87, LEU101, HIS105, LEU108, TYR112, MET115, PRO118, PHE120, ILE145, VAL146, ILE149
BK _{Ca} channels	3NAF	FPD	63.56	No	ARG368	ASP367, ARG368, ASP369, MET513, GLU535, TYR537, ASP601, ALA602, PHE929, ASN930
		CID:5,946 (Tetraethylammonium chloride)	50.71	No	No	ARG368, ASP369, MET513, GLU535, TYR537, ALA602, PHE929, ASN930
VDCC	1T0H	FPD	60.55	No	No	VAL64, ARG65, THR66, ASN67, VAL68, PHE87, TRP104, PRO119, PRO121, LEU124
		CID:4,485 (nifedipine)	78.56	No	No	VAL64, ARG65, THR66, ASN67, VAL68, LEU93, TRP104, ILE118, PRO119, PRO121, LEU124
Angiotensin II receptor 1	4YAY	FPD	63.87	No	TYR92	TYR35, PHE77, TRP84, TYR87, TYR92, VAL108, PRO285, ILE288
		CID:2,541 (candesartan)	132.79	ARG167	No	ALA21, GLY22, ARG23, ILE31, TYR35, PHE77, TRP84, TYR87, THR88, TYR92, SER105, VAL108, ARG167, ILE172, VAL179, ASP281, MET284, PRO285, ILE288

revealed the interactive amino acid residues and binding site conformation of compound FPD docked on the specified targets.

Acute and Sub-acute Oral Toxicity of FPD in Swiss Albino Mice

Acute and sub-acute oral toxicity studies with FPD in Swiss albino mice showed no mortality, morbidity, and no change in gait or posture throughout the experimental period. Blood and serum samples upon analysis did not show any significant changes in the hematological and biochemical parameters studied, and are presented in **Table 3**. Animals on gross pathological examination showed non-significant changes in physical appearances, texture, and absolute and relative weights of vital organs, the details are shown in **Figure 11**. These observations suggested that FPD was well tolerated by Swiss albino mice up to 1,000 mg kg⁻¹ in body weight as a single acute oral dose and up to 100 mg kg⁻¹ as a repeated oral dose for 28 days.

DISCUSSION

The results of the present study demonstrate that 1) FPD produced an antihypertensive response in SHR animals; 2) FPD markedly inhibited Ang II-induced contraction in the rat superior mesenteric artery; 3) the relaxation response to FPD was independent of the endothelium; 4) nevertheless, the test compound increased tissue cGMP levels and the relaxation response elicited with FPD was significantly attenuated by sGC inhibitor ODQ; 5) FPD markedly inhibited L-type calcium channel agonist Bay K8644-induced contractions in

the mesenteric arterial rings, as well as attenuated Bay K8644-stimulated Ca²⁺ influx in aortic smooth muscle cells; 6) BK_{Ca} channel blockers like iberiotoxin (10 nM) and TEA (1 mM) significantly inhibited FPD-induced relaxation in the mesenteric artery; 7) potassium channel opening by FPD was evident from fluorescence studies with VSMCs which showed FPD-induced increase in thallium ion entry and its blockade by TEA (10 mM) and KCl (80 mM); and 8) the test drug was well tolerated by Swiss albino mice up to 1,000 mg kg⁻¹ in acute oral toxicity given as a single dose and up to 100 mg kg⁻¹ in sub-acute oral toxicity when given once daily for 28 days.

Optimization of the substituents around the benzimidazole nucleus has resulted in many drugs including important antihypertensive molecules like candesartan, telmisartan, and cilexetil (**Supplementary Figure S1A**). Many benzimidazole-based compounds act as antihypertensives by intercepting the renin-angiotensin-aldosterone system (RAS) in which angiotensin II (Ang II), by acting on the AT1 receptor, causes vasoconstriction, Na⁺ retention, aldosterone release, and the development of hypertension. The aim of our designed pharmacophore was to obtain a small molecule antihypertensive agent on a benzimidazole core. The lead compound FPD (a C-substituted fluorophenyl benzimidazole) during detailed *ex vivo* studies in healthy Wistar rats showed AT1 receptor blocking activity and modulation of VDCC function, which are greatly affected in *in vivo* models like SHRs, and in line with our hypothesis, the molecule exhibited strong antihypertensive activity in SHRs. The molecule in the present study is much smaller C-substituted fluorophenyl benzimidazole and currently no such report is available on its antihypertensive activity. Recently the synthesis, characterization, and antihypertensive activities of 2-phenyl-substituted benzimidazoles and aminocarbonyl benzimidazoles were reported

TABLE 3 | Effect of FPD as a single acute oral dose at 5, 50, 300, and 1,000 mg kg⁻¹ and as a sub-acute oral dose at 0.1, 1, 10, and 100 mg kg⁻¹ (once orally for 28 days) on body weight and hematological and serum biochemical parameters in Swiss albino mice (mean ± SEM; n = 6).

Parameters	Dose of FPD at mg kg ⁻¹ body weight as a single oral dose				Dose of FPD at mg kg ⁻¹ body weight as a repeated oral dose				
	Control	5 mg kg ⁻¹	50 mg kg ⁻¹	300 mg kg ⁻¹	Control	0.1 mg kg ⁻¹	1 mg kg ⁻¹	10 mg kg ⁻¹	100 mg kg ⁻¹
Body weight (gm)	26.92 ± 1.79	28.00 ± 1.57	25.53 ± 0.95	25.28 ± 2.13	33.70 ± 2.14	32.20 ± 2.95	30.12 ± 0.96	29.45 ± 1.15	29.48 ± 0.60
Hemoglobin (gm dL ⁻¹)	13.11 ± 0.97	14.02 ± 0.57	15.31 ± 0.49	14.77 ± 0.65	16.64 ± 0.65	17.86 ± 0.76	17.20 ± 0.33	17.68 ± 0.68	16.88 ± 0.38
RBC (million mm ⁻³)	6.62 ± 1.02	6.60 ± 0.72	6.61 ± 0.27	6.67 ± 0.81	9.30 ± 1.27	8.97 ± 1.19	9.93 ± 0.35	9.80 ± 0.29	9.86 ± 0.23
WBC (thousands mm ⁻³)	4.56 ± 0.27	5.30 ± 0.55	4.33 ± 0.13	4.85 ± 0.31	4.30 ± 0.23	4.71 ± 0.26	3.78 ± 0.46	4.12 ± 0.44	4.41 ± 0.33
ALP (U L ⁻¹)	343.04 ± 25.44	340.11 ± 62.96	332.99 ± 73.78	340.66 ± 70.62	203.34 ± 5.57	202.06 ± 9.42	208.66 ± 25.58	209.00 ± 8.52	200.82 ± 14.78
SGOT (U L ⁻¹)	22.08 ± 2.41	23.07 ± 2.27	21.35 ± 2.93	27.01 ± 3.56	47.90 ± 10.12	48.82 ± 3.40	42.20 ± 4.54	42.65 ± 6.22	45.65 ± 7.40
SGPT (U L ⁻¹)	22.29 ± 2.14	25.28 ± 2.38	21.35 ± 2.82	20.14 ± 1.16	22.93 ± 1.82	22.77 ± 4.30	18.26 ± 0.76	18.82 ± 0.58	21.08 ± 5.11
Creatinine (mg dl ⁻¹)	0.28 ± 0.01	0.35 ± 0.02	0.30 ± 0.03	0.35 ± 0.02	0.32 ± 0.02	0.37 ± 0.01	0.30 ± 0.01	0.32 ± 0.01	0.31 ± 0.01
Triglycerides (mg dl ⁻¹)	122.87 ± 7.87	135.61 ± 3.74	127.28 ± 4.01	120.09 ± 3.10	81.81 ± 4.75	77.54 ± 9.32	78.14 ± 7.35	78.23 ± 13.96	71.37 ± 3.42
Cholesterol (mg dl ⁻¹)	141.37 ± 4.75	136.06 ± 8.98	133.31 ± 4.46	144.97 ± 7.06	165.38 ± 17.16	162.17 ± 16.19	169.24 ± 8.65	169.78 ± 6.10	162.95 ± 4.95
Bilirubin (mg dL ⁻¹)	0.37 ± 0.02	0.39 ± 0.02	0.33 ± 0.02	0.39 ± 0.03	0.35 ± 0.01	0.39 ± 0.03	0.34 ± 0.01	0.42 ± 0.03	0.33 ± 0.03
Albumin (g dl ⁻¹)	2.06 ± 0.15	2.38 ± 0.14	2.11 ± 0.09	2.42 ± 0.12	2.76 ± 0.11	2.88 ± 0.06	2.88 ± 0.11	3.22 ± 0.03	2.87 ± 0.02
Protein (mg ml ⁻¹)	5.93 ± 0.42	6.44 ± 0.25	6.77 ± 0.25	6.96 ± 0.24	6.06 ± 0.27	6.28 ± 0.19	5.78 ± 0.16	6.39 ± 0.28	5.59 ± 0.05

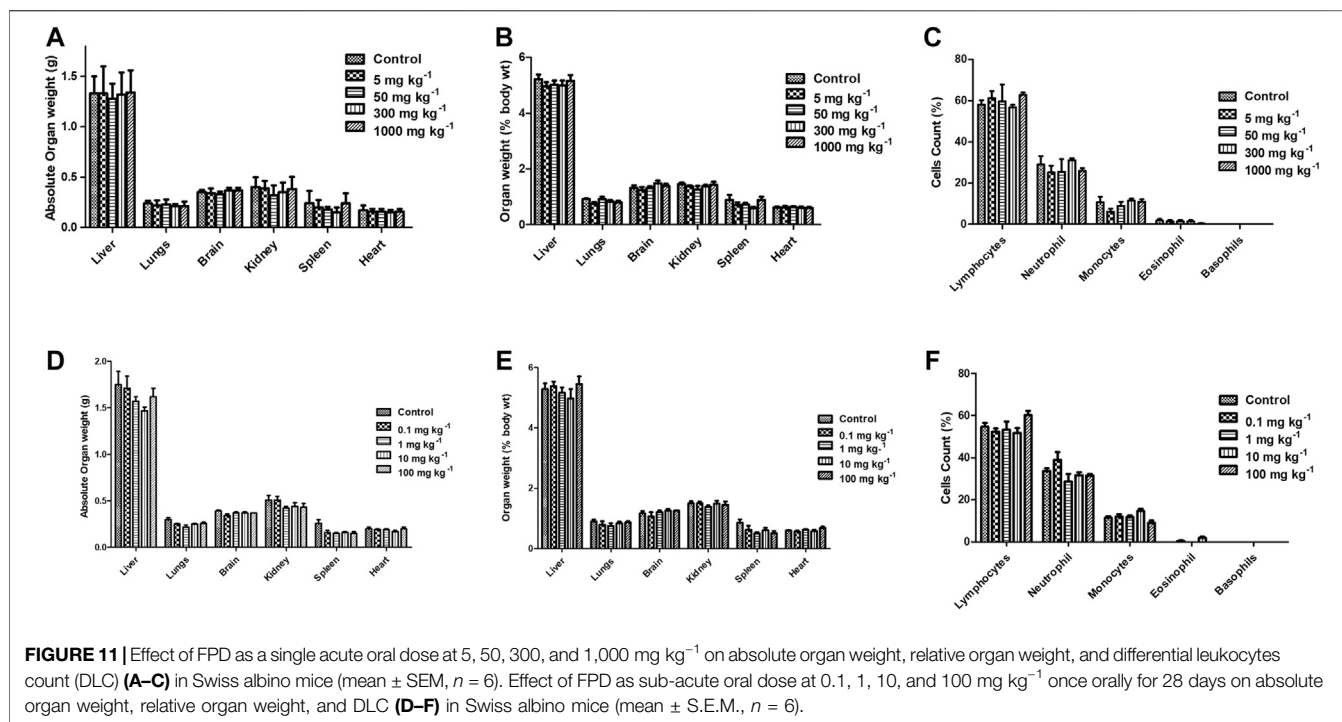
(Khan et al., 2018; Wu et al., 2019). The AT1 receptor blocking action of FPD in the rat superior mesenteric artery, as demonstrated in the present investigation, appears to be consistent with its antihypertensive action in an SHR model of hypertension. In agreement with our observations, the antihypertensive activity and AT1 receptor blocking activity of benzimidazoles like candesartan (Nagai et al., 2004) and substituted benzimidazoles like 5-nitro benzimidazoles (Shah et al., 2008), and 1, 4 or 1, 5 di-substituted benzimidazoles (Zhu et al., 2014) were also reported. SHR are known to have a very high level of angiotensin II expression and downstream AT1 receptor activation for the induction of high blood pressure (Mao and Li, 2015) and hence AT1 receptor blockers were found to be the most frequently reported antihypertensive agent in these models (Choisy et al., 2015).

Regarding the contribution of the vascular endothelium, the observations of the present study show that FDP-induced relaxation of the superior mesenteric artery was endothelium-independent. Our finding is consistent with an earlier report, which demonstrated endothelium-independent vasodilation response of 2-substituted 1H benzimidazoles in rat aorta (Estrada-Soto et al., 2006).

Intracellular rise in cGMP level in vascular smooth muscle and downstream activation of G kinase are well established mechanisms for vasodilation response, and antihypertensive activity of a number of pharmacophores, including NO and NO donors. Blocking of vasodilation response of FPD by ODQ indicates the involvement of sGC in the smooth muscle relaxation response. This is further supported by the tissue cGMP buildup in mesenteric arteries upon treatment with FPD. Antihypertensive benzimidazoles like candesartan were found to enhance cGMP buildup in heart tissue from an ischemia and reperfusion-induced model of cardiac infarction in mongrel dogs (Jugdutt et al., 2000).

The sensitivity of relaxation response of FPD in superior mesenteric arteries to high K⁺, TEA, and iberiotoxin suggested the involvement of the BK_{Ca} channel in the vasodilation response, which was further confirmed by the observation that TEA and KCl (80 mM) blocked thallium ion entry into aortic smooth muscle cells. Additional evidence for the involvement of BK_{Ca} channels in the vasorelaxation mechanism of FPD comes from the *in silico* studies showing a decent docking score. However, an electrophysiological study with FPD using a patch clamp would provide a more direct evidence of the modulation of BK channel function by FPD. The rise of intracellular cGMP level in vascular smooth muscle and its close association in the functional modulations of the BK_{Ca} channel has been reported by several workers including us (Chanda et al., 2016; Liu et al., 2016).

The present study also identified VDCC as a putative target for FPD contributing to vasorelaxation response in superior mesenteric arteries and also in antihypertensive activity in SHRs. FPD significantly blocked Bay K8644-induced contractile response in a mesenteric artery, and also Bay K8644-stimulated Fluo-4-fluorescence in rat VSMC. Docking studies of FPD with the L-type calcium channel are also in strong agreement with the *ex vivo* and *in vitro* observations. Although literature is available for benzimidazole molecules like NS-649 (Varming et al., 1996) and mibefradil for calcium channel blocking activities, no such reports



are available for fluorophenyl benzimidazoles. Mibefradil, a benzimidazolyl-substituted tetraline analogue, selectively blocks T-type voltage-gated plasma membrane calcium channels in vascular smooth muscle (Ernst and Kelly, 1998; Ball et al., 2009). However, like the BK_{Ca} channel, an electrophysiological study with FPD using a patch clamp would provide direct evidence of the blockade of VDCC by FPD.

In both the acute (FPD 100 mg kg⁻¹ as single acute oral dose) and sub-acute oral toxicity studies in Swiss albino mice (FPD 100 mg kg⁻¹ once daily for 28 days) the test drug did not exhibit any toxicity.

LIMITATIONS

There are certain limitations in the present study. For example, we studied the antihypertensive action of FPD in SHR, but the mechanistic work with respect to vasorelaxant mechanisms were studied in the superior mesenteric artery/aortic smooth muscle cells from Wistar rats. Further, future investigations using patch clamp studies are required to provide direct evidence for the involvement of L-type calcium and BK_{Ca} channels in the vasorelaxation mechanisms of FPD. The aim of the docking study was to determine whether FPD binds with selected targets with a decent docking score as we speculated that FPD binds the selected targets to produce biological activities in *ex vivo*, *in vitro*, and *in vivo* models. However, detailed *in silico* docking of FPD to the selected target proteins at their biologically active pockets may be studied to understand the specific effect of FPD in its targets which were not explored in the present study.

CONCLUSION

The present study demonstrates that FPD (C-fluorophenyl benzimidazole), a novel AT₁ receptor blocker possessed antihypertensive activity in the SHR hypertension model. It is also suggested that an FPD-induced rise in tissue cGMP, blockade of L-type calcium channels, and opening of BK_{Ca} channels may significantly contribute to the vasorelaxation mechanisms.

DATA AVAILABILITY STATEMENT

The raw data supporting the conclusions of this article will be made available by the authors, without undue reservation.

ETHICS STATEMENT

The animal study was reviewed and approved by the Institutional Animal Ethics Committee of CSIR-CIMAP, Lucknow, under the central agency CPCSEA, Government of India.

AUTHOR CONTRIBUTIONS

DC designed the study and wrote manuscript. HI performed the research, analyzed the data and wrote the manuscript. PY, DM performed the research and analysed the data. AV and AN performed chemical synthesis of analogues. SA and Fk performed and analysed *in-silico* research and data. MS, KH, HI, and PY performed SHR experiments.

FUNDING

We received seed grant for the research during 2014–2017 by DST and till 2019 by CSIR and the funds have been exhausted. Received no money for open access publication. Ms HI received Senior research fellowship during 2015–2019 for her doctoral program from UGC, Govt of India.

ACKNOWLEDGMENTS

The authors acknowledge the Department of Science and Technology (Grant Nos. SB/YS/LS-40/2014–2017), CSIR (Grant Nos. HCP0010), New Delhi, India, and Director, CSIR-

CIMAP, Lucknow, UP, India for financial assistance. We also acknowledge SRF from UGC, Govt of India to HI. The authors are grateful to Santosh K. Mishra, ex-principal scientist, IVRI, Bareilly, UP, India and Phil Aaronson, reader, Division of AALB, School of Medicine, King's College, London, United Kingdom for their critical review and comments on the manuscript.

SUPPLEMENTARY MATERIAL

The Supplementary Material for this article can be found online at: <https://www.frontiersin.org/articles/10.3389/fphar.2021.611109/full#supplementary-material>.

REFERENCES

- Alam, S., and Khan, F. (2019). 3D-QSAR, Docking, ADME/Tox studies on Flavone analogs reveal anticancer activity through Tankyrase inhibition. *Sci. Rep.* 9 (1), 5414. doi:10.1038/s41598-019-41984-7
- Alam, S., and Khan, F. (2018). QSAR, docking, ADMET, and system pharmacology studies on tormentic acid derivatives for anticancer activity. *J. Biomol. Struct. Dyn.* 36 (9), 2373–2390. doi:10.1080/07391102.2017.1355846
- Alam, S., Nasreen, S., Ahmad, A., Darokar, M. P., and Khan, F. (2020). Detection of natural inhibitors against human liver cancer cell lines through QSAR, Molecular Docking, and ADMET studies. *Curr. Top. Med. Chem.* 20, 1. doi:10.2174/1568026620666201204155830
- Alonso, M. J., Rico, I., Salices, M., and Marin, J. (1989). Effects of the Ca agonists Bay K 8644 and CGP 28392 on vascular smooth muscle tone. *Gen. Pharmacol.* 20, 827–831. doi:10.1016/0306-3623(89)90338-8
- Ball, C. J., Wilson, D. P., Turner, S. P., Saint, D. A., and Beltrame, J. F. (2009). Heterogeneity of L- and T-channels in the vasculature: rationale for the efficacy of combined L- and T-blockade. *Hypertension* 53 (4), 654–660. doi:10.1161/HYPERTENSIONAHA.108.125831
- Bansal, Y., and Silakari, O. (2012). The therapeutic journey of benzimidazoles: a review. *Bioorg. Med. Chem.* 20, 6208–6236. doi:10.1016/j.bmc.2012.09.013
- Chanda, D., Prieto-Lloret, J., Singh, A., Iqbal, H., Yadav, P., Snetkov, V., et al. (2016). Glabridin-induced vasorelaxation: evidence for a role of BKCa channels and cyclic GMP. *Life Sci.* 165, 26–34. doi:10.1016/j.lfs.2016.09.018
- Chanda, D., Shanker, K., Pal, A., Luqman, S., Bawankule, D. U., Mani, D., et al. (2009). Safety evaluation of trikatu, a generic ayurvedic medicine in charles foster rats. *J. Toxicol. Sci.* 34, 99–108. doi:10.2131/jts.34.99
- Chaturvedi, A. K., Verma, A. K., Thakur, J. P., Roy, S., Bhushan Tripathi, S., Kumar, B. S., et al. (2018). A novel synthesis of 2-arylbenzimidazoles in molecular sieves-MeOH system and their antitubercular activity. *Bioorg. Med. Chem.* 26 (15), 4551–4559. doi:10.1016/j.bmc.2018.07.049
- Cheng, Y. Q., Tan, B. Y., Yu, X. H., Dong, W. Z., Su, D. F., Zhu, D. Q., et al. (2018). Synergism of amlodipine and candesartan on blood pressure reduction and organ protection in hypertensive rats. *Clin. Exp. Pharmacol. Physiol.* 45 (6), 514–524. doi:10.1111/1440-1681.12901
- Choisy, S. C., Kim, S. J., Hancox, J. C., Jones, S. A., and James, A. F. (2015). Effects of candesartan, an angiotensin II receptor type I blocker, on atrial remodeling in spontaneously hypertensive rats. *Physiol. Rep.* 3 (1), e12274. doi:10.14814/phy2.12274
- Das, A., Gangarde, Y. M., Tomar, V., Shinde, O., Upadhyay, T., Alam, S., et al. (2020). Small-molecule inhibitor prevents insulin fibrillogenesis and preserves activity. *Mol. Pharm.* 17 (6), 1827–1834. doi:10.1021/acs.molpharmaceut.9b01080
- Ernst, M. E., and Kelly, M. W. (1998). Mibefradil, a pharmacologically distinct calcium antagonist. *Pharmacotherapy* 18 (3), 463–485. doi:10.1002/j.1875-9114.1998.tb03110.x
- Estrada-Soto, S., Villalobos-Molina, R., Aguirre-Crespo, F., Vergara-Galicia, J., Moreno-Díaz, H., Torres-Piedra, M., et al. (2006). Relaxant activity of 2-(substituted phenyl)-1H-benzimidazoles on isolated rat aortic rings: design and synthesis of 5-nitro derivatives. *Life Sci.* 79 (5), 430–435. doi:10.1016/j.lfs.2006.01.019
- Jain, M., Iqbal, H., Yadav, P., Singh, H., Chanda, D., Jagavelu, K., et al. (2020). Autophagy inhibition by chloroquine prevents increase in blood pressure & preserves endothelial functions. *Trop. J. Pharm. Res.* 19, 789–796. doi:10.4314/tjpr.v19i4.16
- Jugdutt, B. I., Xu, Y., Balghith, M., Moudgil, R., and Menon, V. (2000). Cardioprotection induced by AT1R blockade after reperfused myocardial infarction: association with regional increase in AT2R, IP3R and PKCepsilon proteins and cGMP. *J. Cardiovasc. Pharmacol. Ther.* 5 (4), 301–311. doi:10.1054/JCPT.2000.19245
- Khan, M. T., Razi, M. T., Jan, S. U., Mukhtiar, M., Gul, R., Hussain, A., et al. (2018). Synthesis, characterization and antihypertensive activity of 2-phenyl substituted benzimidazoles. *Pak. J. Pharm. Sci.* 31, 1067–1074. doi:10.17582/journal.pjar/2018/31.4.390.395
- Liu, T., Schroeder, H. J., Zhang, M., Wilson, S. M., Terry, M. H., Longo, L. D., et al. (2016). S-nitrosothiols dilate the mesenteric artery more potently than the femoral artery by a cGMP and L-type calcium channel-dependent mechanism. *Nitric Oxide* 58, 20–27. doi:10.1016/j.niox.2016.05.006
- Lloyd, J., Finlay, H. J., Atwal, K., Kover, A., Prol, J., Yan, L., et al. (2009). Dihydropyrazolopyrimidines containing benzimidazoles as K(V)1.5 potassium channel antagonists. *Bioorg. Med. Chem. Lett.* 19, 5469–5473. doi:10.1016/j.bmlcl.2009.07.083
- Mao, S., and Li, C. (2015). Hypotensive and angiotensin-converting enzyme inhibitory activities of *Eisenia fetida* extract in spontaneously hypertensive rats. *Evid. Based Complement. Altern. Med.* 2015, 349721. doi:10.1155/2015/349721
- Nagai, M., Horikoshi, K., Izumi, T., Seki, S., Taniguchi, M., Taniguchi, I., et al. (2004). Cardioprotective action of perindopril versus candesartan in renovascular hypertensive rats. *Cardiovasc. Drugs Ther.* 18 (5), 353–362. doi:10.1007/s10557-005-5059-7
- Prieto-Lloret, J., Snetkov, V. A., Shaifta, Y., Docio, I., Connolly, M. J., MacKay, C. E., et al. (2018). Role of reactive oxygen species and sulfide-quinone oxoreductase in hydrogen sulfide-induced contraction of rat pulmonary arteries. *Am. J. Physiol. Lung Cell Mol. Physiol.* 314 (4), L670–L685. doi:10.1152/ajplung.00283.2016
- Rizzoni, D., Porteri, E., Bettoni, G., Piccoli, A., Castellano, M., Muiesan, M. L., et al. (1998). Effects of candesartan cilexetil and enalapril on structural alterations and endothelial function in small resistance arteries of spontaneously hypertensive rats. *J. Cardiovasc. Pharmacol.* 32 (5), 798–806. doi:10.1097/00005344-199811000-00017
- Shah, D. I., Sharma, M., Bansal, Y., Bansal, G., and Singh, M. (2008). Angiotensin II—AT1 receptor antagonists: design, synthesis and evaluation of substituted carboxamido benzimidazole derivatives. *Eur. J. Med. Chem.* 43 (9), 1808–1812. doi:10.1016/j.ejmech.2007.11.008
- Singh, A., Kumar, B. S., Iqbal, H., Alam, S., Yadav, P., Verma, A. K., et al. (2019). Antihypertensive activity of diethyl-4,4'-dihydroxy-8,3'-neolign-7,7'-dien-9,9'-dionate: a

- continuation study in L-NAME treated wistar rats. *Eur. J. Pharmacol.* 858, 172482. doi:10.1016/j.ejphar.2019.172482
- Singh, A., Kumar, B. S., Alam, S., Iqbal, H., Khan, M. F., Negi, A. S., et al. (2017). Diethyl-4,4'-dihydroxy-8,3'-neolign-7,7'-dien-9,9'-dionate exhibits antihypertensive activity in rats through increase in intracellular cGMP level and blockade of calcium channels. *Eur. J. Pharmacol.* 799, 84–93. doi:10.1016/j.ejphar.2017.01.044
- Varming, T., Christophersen, P., Møller, A., Peters, D., Axelsson, O., and Nielsen, E. Ø. (1996). Synthesis and biological activity of the neuronal calcium channel blocker 2-amino-1-(2,5-dimethoxyphenyl)-5-trifluoromethyl benzimidazole (NS-649). *Bioorg. Med. Chem. Lett.* 6, 245–248. doi:10.1016/0960-894x(96)00010-8
- Weber, S. C., Gratopp, A., Akanbi, S., Rheinlaender, C., Sallmon, H., Barikbin, P., et al. (2011). Isolation and culture of fibroblasts, vascular smooth muscle, and endothelial cells from the fetal rat ductus arteriosus. *Pediatr. Res.* 70, 236–241. doi:10.1203/PDR.0b013e318225f748
- WHO (2017). *WHO fact sheets: cardiovascular diseases*. Geneva, Switzerland: WHO.
- Woolley, D. W. (1944). Some biological effects produced by benzimidazole & their reversal by purines. *J. Biol. Chem.* 152, 225–232. doi:10.1016/s0021-9258(18)72045-0
- Wu, Z., Anh, N. T. P., Yan, Y. J., Xia, M. B., Wang, Y. H., Qiu, Y., et al. (2019). Design, synthesis and biological evaluation of AT1 receptor blockers derived from 6-substituted aminocarbonylbenzimidazoles. *Eur. J. Med. Chem.* 181, 111553. doi:10.1016/j.ejmech.2019.07.056
- Zhu, W., Da, Y., Wu, D., Zheng, H., Zhu, L., Wang, L., et al. (2014). Design, synthesis and biological evaluation of new 5-nitro benzimidazole derivatives as AT1 antagonists with anti-hypertension activities. *Bioorg. Med. Chem.* 22 (7), 2294–2302. doi:10.1016/j.bmc.2014.02.008

Conflict of Interest: The authors declare that the research was conducted in the absence of any commercial or financial relationships that could be construed as a potential conflict of interest.

Copyright © 2021 Iqbal, Verma, Yadav, Alam, Shafiq, Mishra, Khan, Hanif, Negi and Chanda. This is an open-access article distributed under the terms of the Creative Commons Attribution License (CC BY). The use, distribution or reproduction in other forums is permitted, provided the original author(s) and the copyright owner(s) are credited and that the original publication in this journal is cited, in accordance with accepted academic practice. No use, distribution or reproduction is permitted which does not comply with these terms.